Chinese Chemical Letters 34 (2023) 107654

Contents lists available at ScienceDirect

Chinese Chemical Letters

journal homepage: www.elsevier.com/locate/cclet

Engineering trienzyme cascade-triggered fluorescent immunosensor platform by sequentially integrating alkaline phosphatase, tyrosinase and horseradish peroxidase

Yujie Sun[a,1], Lei Wen[b,1], Huili Ma[a,1], Wenlin Ma[a], Zhenqian Fu[a], Yinhui Li[b,*], Chengwu Zhang[c], Lin Li[a], Jinhua Liu[a,*]

[a] Institute of Advanced Materials (IAM), Key Laboratory of Flexible Electronics (KLOFE), Nanjing Tech University, Nanjing 211816, China
[b] Key Laboratory for Green Organic Synthesis and Application of Hunan Province, Key Laboratory of Environmentally Friendly Chemistry, Application of Ministry of Education, College of Chemistry, Xiangtan University, Xiangtan 411105, China
[c] School of Basic Medical Sciences, Shanxi Medical University, Taiyuan 310003, China

ARTICLE INFO

Article history:
Received 3 April 2022
Revised 7 June 2022
Accepted 29 June 2022
Available online 2 July 2022

Keywords:
Enzyme cascade
Alkaline phosphatase
Tyrosinase
Horseradish peroxidase
Cardiac troponin I

ABSTRACT

Mulit-enzyme cascades are a major type of chemical transformations and play a crucial role in biological signal transduction and metabolism. Herein, a trienzyme cascade-triggered fluorescent immunosensor platform was constructed by sequentially integrating alkaline phosphatase (ALP), tyrosinase (TYR) and horseradish peroxidase (HRP). The proposed platform was based on HRP-induced a rapid *in situ* fluorogenic reaction between dopamine (DA) and 1,5-dihydroxynaphthalene (DHA) to produce a strong yellow azamonardine fluorescent compound (AFC). The obtained AFC was clearly characterized by high-resolution mass spectrum, ^{1}H NMR, ^{13}C NMR and theoretical calculations. The integration of the two-enzyme system (TYR and HRP) or three-enzyme system (ALP, TYR and HRP) led to a maximum of 400.0-fold and 250.0-fold fluorescence enhancements, respectively. Using cardiac troponin I (cTnI) as the model antigen, a trienzyme cascade-triggered fluorescent immunosensor platform was developed for quantitative detecting cTnI in a wide linear range from 2 ng/mL to 150 ng/mL with a detection limit of 0.67 ng/mL. In addition, the proposed platform was successfully applied in detection of cTnI in serum of clinical patients. Overall, the developed fluorescent immunosensor performs powerful implications for researching enzyme cascade systems in the field of biomedicine.

Enzyme cascade reactions perform multiple enzymatic reactions in sequence, act as an important part to signal transduction and amplification in biological systems, and also have a wide applicate prospect in biotechnology [1–3]. So far numerous efforts have been exerted for the development of enzyme cascade mechanisms and behaviors on multiple platforms, and there is an increasing interest in developing multi-enzyme cascade system with a new signal generation that integrates multiple biocatalytic conversions [4–6]. Currently, most of the characterization and quantification of enzyme cascade systems are based on specific colorimetric methods, in which alkaline phosphatase (ALP) and horseradish peroxidase (HRP) are commonly employed inducible enzymes [7–9]. Additionally, there are few substrate/product pairs and signal generation patterns in the present system. Therefore, it is of great demand to develop a multi-enzyme cascade with a new signal generation mechanism.

So far various methods for biosensing multi-enzyme cascade-induced reaction have been developed for the application such as colorimetric [10], electrochemical [11], chemiluminescence [12], fluorescence [13]. In spite of some advantages of fluorescence assays, the sensing ways of the enzyme cascade system are limited to the colorimetric due to lack of substrates or products suitable for appropriate application systems [14]. It is attractive to develop fluorogenic substrate of the multi-enzyme cascade systems. For example, Yang group developed an enzyme cascade immunoassay for sensing cTnI based on enzymes-induced fluorogenic and chromogenic reaction by coupling the ALP and tyrosinase (TYR) [15]. Chang group reported a dual-enzyme cascade biosensor for ultrasensitive detection of MicroRNA153 based on self-assembly of copper nanoparticles to enhance fluorescence signal [16]. However, to our knowledge, the so far reported enzyme cascade systems only utilized on two-enzyme strategies and required the abiotic envi-

* Corresponding authors.
E-mail addresses: yinhuili16@163.com (Y. Li), iamjhliu@njtech.edu.cn (J. Liu).
[1] These authors contributed equally to this paper.

https://doi.org/10.1016/j.cclet.2022.06.077
1001-8417/

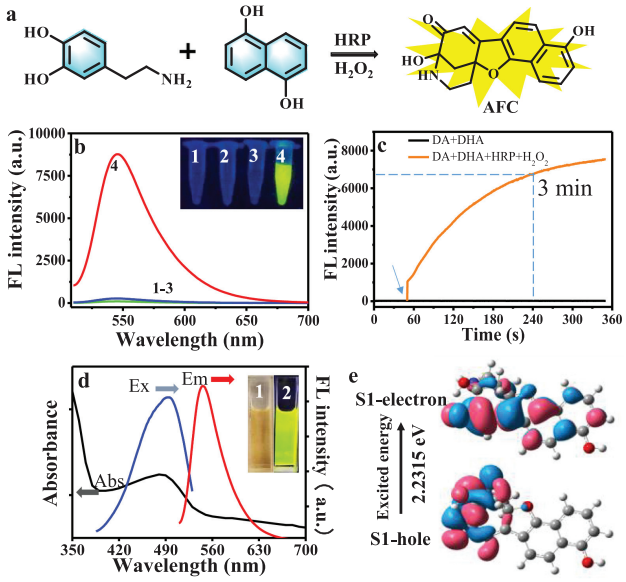

Fig. 1. (a) A mechanism of HRP activity determination based on DA and DHA. (b) Fluorescence emission spectra of DA and DHA: (1) DA + DHA, (2) DA + DHA + H_2O_2, (3) DA + DHA + HRP, (4) DA + DHA + H_2O_2 + HRP. (c) Fluorescence emission-time curves of the DA + DHA (black line), DA + DHA + H_2O_2 + HRP (orange line). (d) Absorption and fluorescence excitation and emission spectral of AFC. The inset shows AFC under natural light and 365 nm UV light, respectively. (e) Calculated excitation energy and natural transition orbital (NTO) of S1 state for AFC.

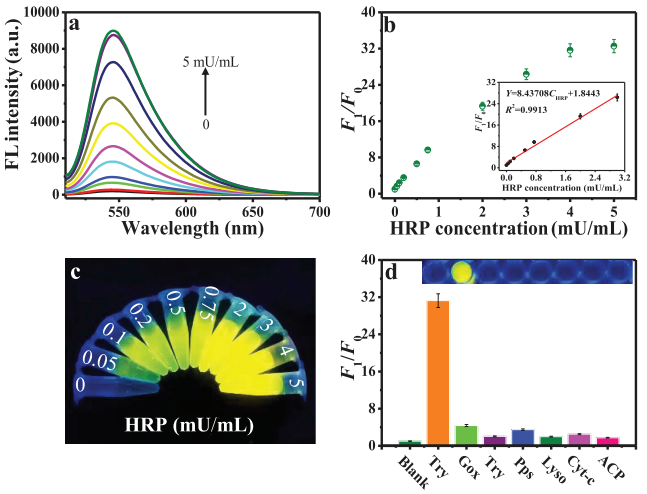

Fig. 2. (a) Fluorescence emission spectra of AFC at different concentrations of HRP at 490 nm excitation. (b) Relationship between the fluorescence intensity ratio (F_1/F_0) and the HRP concentration, inset: linear curve. (c) Corresponding photographs under 365 nm UV light. (d) Selectivity investigation of the sensing system for HRP activity.

ronment. But in the biological system, the enzyme cascade reaction often requires more than two enzymes. Additionally, the substrate of the enzyme is not only intramolecular interaction, but also consists of the interaction of many substances. Therefore, the development of a multi-enzyme cascade system with new fluorescent substrates under a simulated natural environment is necessary.

Herein, we constructed a trienzyme cascade-triggered fluorescent immunosensor platform by sequentially integrating ALP, TYR, and HRP. As reported, DA interacting with resorcinol under neutral conditions would generate a strong fluorescent azamonardine with pale yellow color [17,18]. Aroused by this special reaction, we constructed an innovative ALP/TYR/HRP cascade reaction strategy. The expected ALP catalyzed the cleavage of the phosphate group in PAPP, inducing the conversion of PAPP to tyramine, which was oxidized by TYR to DA. HRP and H_2O_2 promoted the rapid *in-situ* fluorescence reaction of DA and DHA to produce an AFC with a fluorescence quantum yield of 10.2% (Fig. 1a). The optical properties of AFC were investigated by UV-vis absorption and FL spectroscopy. The mixture of DA-DHA-HRP-H_2O_2 showed a strong emission peak around 550 nm with a broad profile, while other mixtures of DA-DHA, DA-DHA-HRP, DA-DHA-H_2O_2 had negligible fluorescence (Fig. 1b and Fig. S2 in Supporting information). Thus, a fluorescent immunosensor platform was constructed based on the special fluorescence reaction of DA and DHA triggered by a trienzyme cascade integrated with ALP, TYR and HRP.

To get the best conditions for generating AFC, the reaction time, pH and precursors concentrations were carefully optimized. As shown in Fig. 1c, the reaction system reached stability in 3 min. Thus, the incubation time was selected for 3 min to obtain AFC in the following experiment. The pH of 7.4 was adopted for subsequent experiments (Fig. S3 in Supporting information). Then, the influence of precursors concentrations was also optimized (Figs. S4-S7 in Supporting information) and the concentrations of DA, DHA, H_2O_2 and tyramine were selected to be 400 μmol/L, 30 μmol/L, 60 μmol/L and 200 μmol/L for the next experiment, respectively.

AFC could be synthesized in the presence of HRP and H_2O_2. The optical properties of AFC were investigated by absorption and fluorescence spectra. As shown in Fig. 1d, AFC exhibited an absorption peak at 490 nm and bright yellow fluorescence under UV light (inset image of Fig. 1d). The excitation and emission wavelength of AFC were fixed at 490 nm and 550 nm, respectively, which indicated a stoke shift of about 60 nm. Furthermore, by theoretical calculations, the emission peak around 550 nm of AFC could be attributed to the parital charge transfer character of the lowest singlet excited state (S1) that demonstrated by the natural transition orbital (NTO) (Fig. 1e). The chemical structure of AFC was characterized and confirmed through ^{1}H NMR, ^{13}C NMR and high-resolution mass spectra (Figs. S8-S10 in Supporting information). Additionally, a possible reaction mechanism for the formation of AFC was proposed (Scheme S1 in Supporting information). Firstly, in the presence of oxygen, DA could be oxidized to an *o*-quinone structure, intermolecular Michael 1,4-addition further happened between the *o*-quinone structure and DHA to give intermediate **b**. Then, coupling product **c** was formed because of the rearomatization of **b**, however, **c** was prone to be oxidized to quinone **d**, and subsequently, the furan-fused intermediate **e** was given though intramolecular Michael addition, the enolate structure of **e** could be also rearranged to its ketone form. Finally, an intramolecular condensation of amino and carbonyl occurred and formed the final product AFC. It was worth noting that the oxidant of atmospheric oxygen was precondition to light the oxidation of catechol to form the strongly emissive chromo-fluorophore AFC.

Under the combined action of HRP and H_2O_2, *in-situ* cyclization occurred between DA and DHA along with a significant fluorescence signal. Inspired by the reaction system and obvious signal output, we successfully achieved high sensitivity and selective monitoring of HRP activity. As shown in Fig. 2a, the fluorescence spectra of the AFC harmonized with the activity of HRP (0 to 5 mU/mL). A maximum of 32-fold signal enhancement was observed when the activity of HRP was up to 5 mU/mL. Meanwhile, it showed a good linear relationship ($F_1/F_0 = 1.8443 + 8.43708C_{HRP}$, $R^2 = 0.99131$) between the fluorescence intensity ratios (F_1/F_0) at 550 nm and the HRP activities (Fig. 2b). The LOD of our method was calculated to be 0.017 mU/mL, which was lower than reported ones by others (Table S1 in Supporting information) [19–22]. Furthermore, obvious fluorescent color changes could be easily

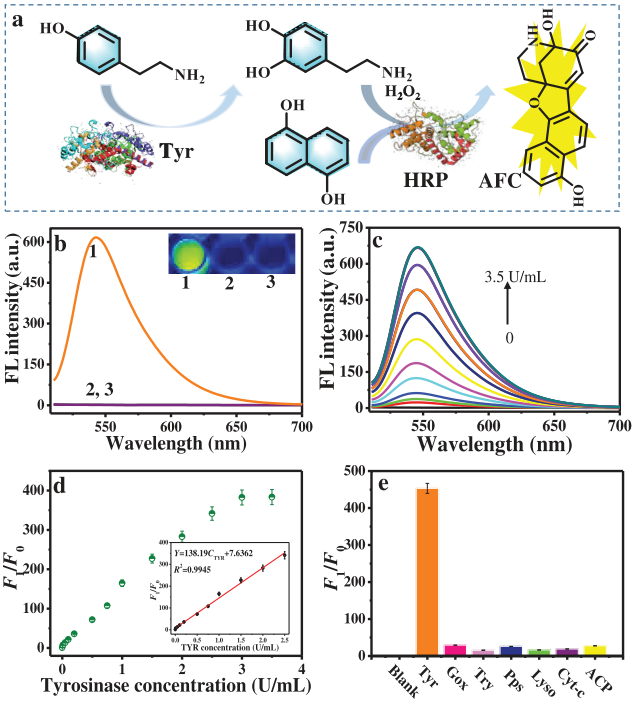

Fig. 3. (a) Mechanism of TYR activity determination based on DA and DHA. (b) Fluorescence emission spectra of tyramine and TYR: (1) tyramine + DHA + H_2O_2 + HRP, (2) TYR + DHA + H_2O_2 + HRP, (3) tyramine + TYR + DHA + H_2O_2 + HRP. (c) Fluorescence emission spectra at different TYR concentrations excited at 490 nm. (d) Relationship between the fluorescence intensity ratio (F_1/F_0) and the TYR concentration, inset: linear curve. (e) Selectivity investigation of the sensing system for TYR activity.

read under ultraviolet light when the HRP concentration was 0.05 mU/mL (Fig. 2c). Additionally, other non-specific proteins/enzymes were selected to clarify the specificity of the developed HRP sensing system, which include GOx, Pepsin, Cyt c, lysozyme, TYR, ACP. Neither of them could cause significant changes in fluorescence signals (Fig. 2d), suggesting the specificity of our sensing system toward HRP. Additionally, we also measure the catalytic activity of the HRP, the Michaelis-Menten constant (K_m) and V_{max} based on the Michaelis-Menten kinetic equation were determined by the saturation curves (Fig. S12 in Supporting information) [23,24]. H_2O_2 was selected as the substrate to test the peroxidase-mimicking activity of HRP. The K_m and V_{max} were 0.28 mmol/L and 4.51×10^{-8} mol L^{-1} s^{-1}, which was lower than those for HRP (Table S1) [25].

TYR could catalyze the hydroxylation of monophenols into catechols [26,27]. Using tyramine as the substrate, TYR catalyzed the hydroxylation of tyramine to DA. DA together with DHA could generate significant fluorescence signals in the presence of HRP and H_2O_2. Such enzyme cascade fluorogenic reaction prompted us to construct an *in situ* fluorescence sensor for TYR activity (Figs. 3a and b). The fluorescence spectra showed concentration-dependent enhancement with increasing TYR activity from 0 to 3.5 U/mL (Fig. 3c). A good linear relationship ($Y = 7.6362 + 138.19C_{tyrosinase}$, $R^2 = 0.9945$) between F_1/F_0 and the TYR activities (0.01 U/mL to 2.5 U/mL) was achieved with a LOD of 3.33 mU/mL. A maximum of 400-fold signal enhancement was observed when the activity of TYR was up to 3.5 U/mL (Fig. 3d). The sensor exhibitd a comparable detection ability with the previously reported TYR sensing methods in Table S1 [28–32]. To prove the specificity of the sensor, non-specific proteins/enzymes including GOx, ACP, Pepsin, lysozyme, trypsin, Cyt c were chosen as interfering substances. These interfering substances did not cause significant signal changes (Fig. 3e), suggesting that our sensor had good selectivity for TYR.

Furthermore, a trienzyme cascade fluorescence sensor using PAPP as substrate to detect ALP activity was developed (Fig. 4a and Fig. S10 in Supporting information). The proposed sensor was based on the ALP-catalyzed the conversion of PAPP to intermediate tyramine; TYR-catalyzed hydroxylation of tyramine to DA, and the specific reaction between DA and DHA in the HRP-H_2O_2 system. As shown in Figs. 4b and c, the fluorescence spectra changed with increasing activity of ALP (0 to 1500 mU/mL). Particular, a good linear relationship between fluorescence intensities ratios (F_1/F_0) at 550 nm and the ALP concentrations (0.05-20 mU/mL and 20-1250 mU/mL) was achieved, and the fitted linear equation could be depicted as $Y_1 = 142.52 + 1.7822C_{ALP}$ (mU/mL), ${R_1}^2 = 0.9929$, $Y_2 = 84.733 + 0.1124C_{ALP}$ (mU/mL), ${R_2}^2 = 0.9723$, respectively. A maximum of 250-fold signal enhancement was observed when the activity of ALP was up to 1.25 U/mL. Therefore, the proposed sensor could be used to detect ALP as low as 0.017 mU/mL. Compared with previously reported methods for ALP measurement (Table S2 in Supporting information) [33–39], the present method had a wider detection range and lower detection limit. Additionally, other non-specific proteins/enzymes were chosen to further study the specificity of our method. None of them produced a significant fluorescence signal except ALP (Fig. 4d). These results suggested that our approach exhibited high sensitivity and excellent selectivity for ALP. Additionally, the K_m and V_{max} of TYR and ALP based on the Michaelis-Menten kinetic equation were determined by the saturation curves, in which tyramine and PAPP were selected as the substrate of TYR and ALP to test the their activity, respectively. Finally, the K_m and V_{max} were 0.58 mmol/L and 6.79×10^{-8} mol L^{-1} s^{-1} for TYR and 0.53 mmol/L and 3.44×10^{-8} mol L^{-1} s^{-1} for ALP (Figs. S13 and S14 in Supporting information).

Ctni, a special myocardial regulatory protein, is considered the gold standard for the early diagnosis of acute myocardial infarction (AMI) [40,41]. Sensitively detecting of cTnI was essential for the diagnosis of AMI. Stimulated by the wide applications of ALP in conventional ELISA, we wanted to apply the enzyme cascade reactions to the cascade ELISA in biomedicine. Based on the above results and using cTnI as a model, we developed a trienzyme cascade-triggered fluorescent immunosensor platform by sequential integrating ALP, TYR, and HRP. It schematically showed the immunological recognition process of the developed cascade ELISA for determination of cTnI (Fig. 5a). Fig. 5b showed the change of cTnI-concentration dependent fluorescence spectra. And Fig. 5c elucidated that the fluorescence intensity at 550 nm increased gradually with the cTnI concentrations (0-150 ng/mL), exhibiting a good linearity with cTnI concentrations (2 ng/mL to 150 ng/mL), and the regression equation could be depicted as $Y_1 = 1.010 + 0.023C_{cTnI}$ (ng/mL), ${R_1}^2 = 0.9743$, $Y_2 = 1.3573 + 0.0092C_{cTnI}$ (ng/mL), ${R_2}^2 = 0.9915$, respectively. The LOD of our method was calculated to be 0.67 ng/mL, which was lower than those previously reported (Table S4 in Supporting information) [42–49]. Furthermore, to prove the specificity of the developed immunosensor, other non-specific proteins, including BSA, AFP, lysozyme and trypsin, were tested in developed fluorescent ELISA, and none of them caused significant signal change (Fig. 5d), suggesting that the developed immunosensor exhibited good selectivity toward cTnI. Therefore, our proposed trienzyme cascade-triggered fluorescent ELISA could be applied to detect cTnI with high sensitivity and selectivity.

The serum is a highly complex biological liquid, which contains a large number of proteins and other interfering molecules. Consequently, identifying biomarkers in serum is very challenging. Encouraged by the excellent selectivity and sensitivity of our pro-

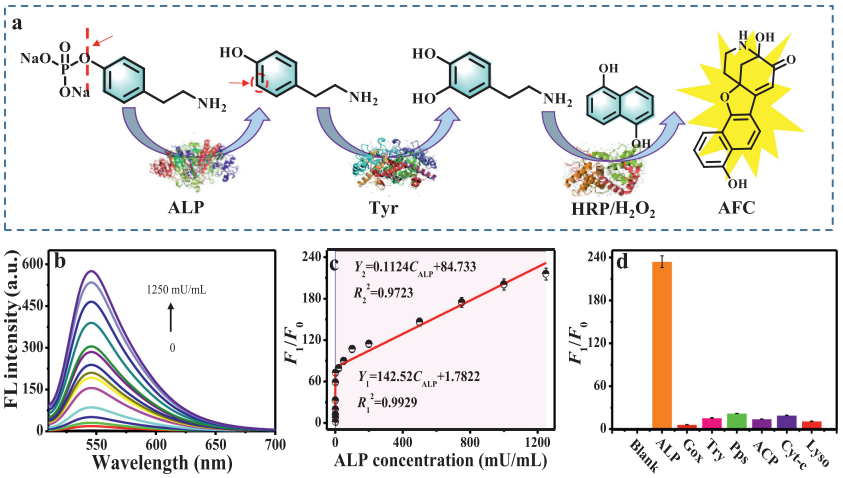

Fig. 4. (a) Mechanism of ALP activity determination based on the ALP-TYR-HRP cascade-triggered fluorogenic reactions. (b) Fluorescence emission spectra at different ALP concentrations excited at 490 nm. (c) Relationship between the fluorescence intensity ratio (F_1/F_0) and the ALP concentration, inset: linear curve. (d) Selectivity investigation of the sensing system for ALP activity.

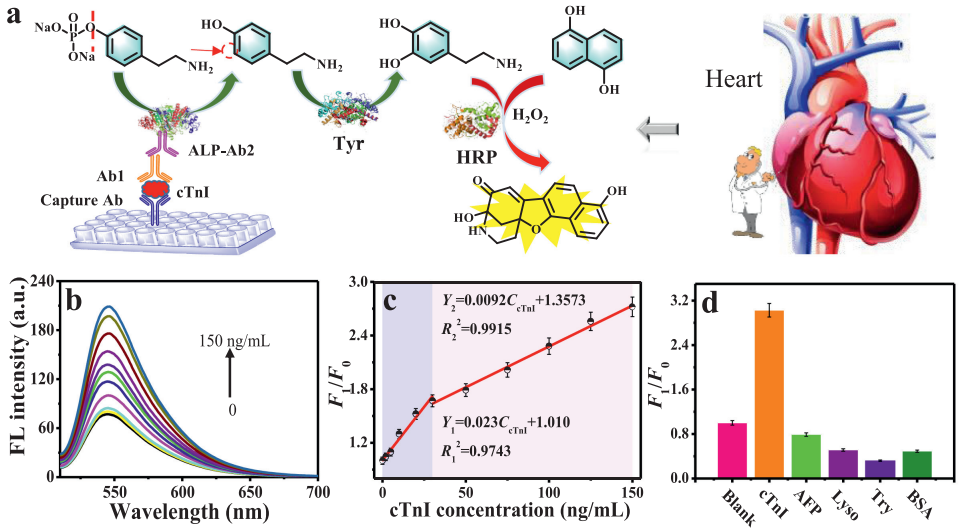

Fig. 5. (a) Schematic representation of the cascade ELISA strategy *via* enzymatic fluorogenic reactions. (b) Fluorescence emission spectra at different cTnI concentrations excited at 490 nm. (c) Relationship between the fluorescence intensity ratio (F_1/F_0) and the cTnI concentration, inset: linear curve. (d) Selectivity investigation of the cascade ELISA system against cTnI or other control enzymes/proteins.

posed trienzyme fluorescent immunosensor, we further applied it to determinate cTnI in actual clinical serum samples. The cTnI levels in six clinical patient samples were measured using our ALP-based ELISA detection system and with commercial standard ELISA kits as control (Table S6 in Supporting information). Noteworthy, the cTnI concentration determined with our system was consistent with the results of the commercial TMB-based standard ELISA kit. It was further proved that the developed assay showed high cTnI evaluation ability in actual clinical samples. It exhibits excellent application prospects in the clinical diagnosis of disease biomarkers.

In summary, we developed a rational trienzyme cascade-triggered fluorescent immunosensor platform by sequential integrating ALP, TYR and HRP. Our proposed approach displayed the following advantages: (i) A pair of new substrates (DA and DHA) for HRP-H_2O_2 system was found, and they could produce a strong yellow azamonardine fluorescent compound (AFC) by a rapid *in situ* fluorogenic reaction. (ii) The obtained AFC was clearly characterized by high-resolution mass spectrum, ^{1}H NMR, ^{13}C NMR and theoretical calculations. (iii) This was the first attempt to develop multi-enzyme cascade sensor system with three enzymes and new substrates (DA and DHA) of HRP. (iv) The integration of the two-enzyme system (TYR and HRP) or three-enzyme system (ALP, TYR and HRP) led to a maximum of 400.0-fold and 250.0-fold enhancements in the activity of the catalytic cascades, respectively, compared with the 32.0-fold enhancement of one-enzyme system (HRP). (v) Compared with the traditional commercial ALP-labeled fluorescent ELISA, our developed fluorescent immunoassay had a wider dynamic detection range from 2-150 ng/mL and lower LOD of 0.67 ng/mL toward cTnI. (vi) The proposed method was successfully applied to the evaluation of cTnI levels in clinical serum samples with satisfied results. Therefore, present study gets over the limitations of a single enzyme and two enzymes in the traditional enzyme cascade reaction. It paves a new way to construct enzyme cascade systems, and gets broad application prospects in the fields of biosensing.

Declaration of competing interest

There are no conflicts of interest.

Acknowledgments

The authors acknowledge the National Natural Science Foundation of China (Nos. 22174065, 21974119), the Science and Technology Planning Project of Hunan Province (No. 2020RC3046) and Hunan Provincial Natural Science Foundation of China (No. 2019JJ30020).

Supplementary materials

Supplementary material associated with this article can be found, in the online version, at 10.1016/j.cclet.2022.06.077.

References

[1] C.W. Chiang, X. Liu, J. Sun, et al., Nano Lett. 20 (2020) 1383–1387.
[2] W. Zhang, L. Liu, Y. Liao, et al., Chin. Chem. Lett. 33 (2022) 334–338.
[3] A. Kuchler, M. Yoshimoto, S. Luginbuhl, F. Mavelli, P. Walde, Nat. Nanotechnol. 11 (2016) 409–420.
[4] M. Castellana, M.Z. Wilson, Y. Xu, et al., Nat. Biotechnol. 32 (2014) 1011–1018.
[5] L. Zhu, X. Zhang, R. Yuan, Y Chai, Anal. Chem. 94 (2022) 1264–1270.
[6] T.H. Kim, P. Mehrabi, Z. Ren, et al., Science 355 (2017) 262.
[7] X. Sun, Y. Li, Q. Yang, et al., Chin. Chem. Lett. 32 (2021) 1780–1784.
[8] S. Tsitkov, H. Hess, ACS Catal. 9 (2019) 2432–2439.
[9] J. Wu, X. Wang, Q. Wang, et al., Chem. Soc. Rev. 48 (2019) 1004–1076.
[10] Y. Liu, R. Lv, S. Sun, et al., Chin. Chem. Lett. 33 (2022) 807–811.
[11] P. Liu, X. Qian, X. Li, et al., ACS Appl. Mater. Inter. 12 (2020) 45648–45656.
[12] Q. Song, X. Yan, H. Cui, M. Ma, ACS Nano 14 (2020) 3696–3702.
[13] Y. Ma, Y. Zhao, N.K. Bejjanki, et al., ACS Nano 13 (2019) 8890–8902.
[14] Y. Guo, X. Li, Y. Dong, G.L. Wang, ACS Sustain. Chem. Eng. 7 (2019) 7572–7579.
[15] J. Zhao, S. Wang, S. Lu, et al., Anal. Chem. 90 (2018) 7754–7760.
[16] J. Cui, H. Han, J. Piao, et al., ACS Appl. Mater. Inter. 12 (2020) 34130–34136.
[17] J. Zhao, X. Bao, S. Wang, et al., Anal. Chem. 89 (2017) 10529–10536.
[18] A.U. Acuna, M. Alvarez-Perez, M. Liras, P.B. Coto, F. Amat-Guerri, Phys. Chem. Chem. Phys. 15 (2013) 16704–16712.
[19] X. Cheng, L. Sun, R. Li, et al., Mikrochim. Acta 186 (2019) 731.
[20] F. Chen, Z. Lin, Y. Zheng, et al., Anal. Chim. Acta 739 (2012) 77–82.
[21] S.V. Kergaravat, M.I. Pividori, S.R. Hernandez, Talanta 88 (2012) 468–476.
[22] P.S. Pidenko, S.A. Pidenko, Y.S. Skibina, et al., Anal. Bioanal. Chem. 412 (2020) 6509–6517.
[23] Y. Song, S. Lu, J. Hai, et al., Anal. Chem. 93 (2021) 11470–11478.
[24] N. Kitchawengkul, A. Prakobkij, W. Anutrasakda, et al., Anal. Chem. 93 (2021) 6989–6999.
[25] L. Gao, J. Zhuang, L. Nie, et al., Nature Nanotech 2 (2007) 577–583.
[26] L. Chai, J. Zhou, H. Feng, et al., ACS Appl. Mater. Inter. 7 (2015) 23564–23574.
[27] Z. Li, Y.F. Wang, C. Zeng, L. Hu, X.J. Liang, Anal. Chem. 90 (2018) 3666–3669.
[28] Z. Han, J. Shu, Q. Jiang, H. Cui, Anal. Chem. 90 (2018) 6064–6070.
[29] X. Han, S. Li, Z. Peng, A.M. Othman, R. Leblanc, ACS Sens. 1 (2016) 106–114.
[30] L. Wang, Z.F. Gan, D. Guo, et al., Anal. Chem. 91 (2019) 6507–6513.
[31] H. Li, W. Liu, F. Zhang, et al., Anal. Chem. 90 (2018) 855–858.
[32] S. Li, R. Hu, S. Wang, et al., Anal. Chem. 90 (2018) 9296–9300.
[33] J. Zhao, G. Liu, J. Sun, et al., Anal. Chem. 92 (2020) 2316–2322.
[34] X. Yang, Y. Luo, Y. Zhuo, Y. Feng, S. Zhu, Anal. Chim. Acta 840 (2014) 87–92.
[35] X. Wu, X. Li, H. Li, W. Shi, H. Ma, Chem. Commun. 53 (2017) 2443–2446.
[36] A. Hayat, B. Gonca, S. Andreescu, Biosens. Bioelectron. 56 (2014) 334–339.
[37] A. Hayat, S. Andreescu, Anal. Chem. 85 (2013) 10028–10032.
[38] J.L. Ma, B.C. Yin, X. Wu, B.C. Ye, Anal. Chem. 88 (2016) 9219–9225.
[39] L.Y. Jin, Y.M. Dong, X.M. Wu, G.X. Cao, G.L. Wang, Anal. Chem. 87 (2015) 10429–10436.
[40] F. Wang, C. Zhang, Q. Xue, H. Li, Y. Xian, Biosens. Bioelectron. 95 (2017) 21–26.
[41] H. Zhao, E. Su, L. Huang, et al., Chin. Chem. Lett. 33 (2022) 743–746.
[42] G.S. Dorraj, M.J. Rassaee, A.M. Latifi, B. Pishgoo, M.J. Tavallaei, J. Biotechnol. 208 (2015) 80–86.
[43] Q. Wu, Y. Sun, D. Zhang, et al., Biosens. Bioelectron. 96 (2017) 288–293.
[44] G. Liu, J. Zhao, S. Wang, et al., Sens. Actuators B: Chem. 306 (2020) 127583.
[45] M.N. Tsaloglou, A. Jacobs, H. Morgan, Anal. Bioanal. Chem. 406 (2014) 5967–5976.
[46] X. Liu, Y. Wang, P. Chen, et al., ACS Sens. 1 (2016) 1416–1422.
[47] X. Guo, L. Zong, Y. Jiao, et al., Anal. Chem. 91 (2019) 9300–9307.
[48] J. Liu, G. Ruan, W. Ma, et al., Biosens. Bioelectron. 198 (2022) 113823.
[49] J. Wu, D.M. Cropek, A.C. West, S. Banta, Anal. Chem. 82 (2010) 8235–8243.